Letter

Laser-induced thermocapillary flows on a flowing soap film

Yu Zhao and Haitao Xu*
Center for Combustion Energy and School of Aerospace Engineering, Tsinghua University, Beijing 100084, China

(Received 18 September 2023; accepted 16 January 2024; published 8 February 2024)

For a flowing soap film with added surfactants, theoretically there exists symmetric elastic waves due to the elasticity of the soap film that originates from the surface tension change with the film surface area change. However, the symmetric elastic waves remain elusive from experimental observations due to the lack of approaches to stimulate such waves. Here, we propose a focused laser heating method to study the properties of liquid films under symmetric disturbances. The thermocapillary flows caused by the laser-induced Marangoni effect lead to symmetric disturbances in the film thickness without causing antisymmetric disturbances in the film shape. Thus, on flowing soap films with low surfactant concentrations, i.e., with appreciable elasticities, the laser-induced disturbances in the film thickness are propagated by the symmetric elastic waves, and the envelope of the wave fronts forms a shock wave starting from the laser heating point. Interestingly, on flowing soap films with high surfactant concentrations, i.e., vanishingly small elasticities, the laser-induced disturbances in the film thickness remain unchanged and flow with the film without propagating, similar to "laser engraving" on free liquid films.

DOI: 10.1103/PhysRevFluids.9.L022001

Liquid films are common in industrial production [1] and are widely studied in scientific research [2–12]. When a pure-liquid film is disturbed antisymmetrically in shape or symmetrically in thickness, the disturbances can respectively propagate in the form of antisymmetric or symmetric Taylor waves [13]. For a soap film, there is theoretically an additional symmetric wave mode due to the film elasticity resulting from surface tension change with surfactant concentration [14–16].

As shown in Fig. 1(a), the antisymmetric and symmetric Taylor waves propagate disturbances in film shape and thickness at speeds of $v_{AS} = \sqrt{2\sigma/\rho h}$ and $v_S = k\sqrt{\sigma h/2\rho}$, respectively, where σ, ρ, and h are the surface tension, density, and thickness of the liquid film, respectively, and k is the wave number, or the inverse of the wave length [13]. The Taylor waves, which were found when studying films of pure liquids, exist in any liquid film [13,17,18]. Most films we encounter in daily life and in industrial applications are formed by liquid mixtures, in which some ingredients are used to reduce the surface tension of the bulk liquids and are thus called surfactants. The symmetric elastic wave, which also propagates disturbances in film thickness, is unique to films with added surfactants. Its wave speed $v_E = \sqrt{2E/\rho h}$ depends on the film elasticity $E = A(\mathrm{d}\sigma/\mathrm{d}A)$, which describes the change of the surface tension with the relative change of the film surface area A [14–16]. Soap films are a typical example and are widely used in experimental study of such films. Freely flowing soap films are typically of thickness $h \sim 10\,\mu\mathrm{m}$ [19–23], much shorter than the disturbance wave lengths, which means that the propagation of the symmetric Taylor mode can be neglected compared to the antisymmetric mode since $v_S/v_{AS} \sim kh \ll 1$. Thus, a challenge in experiments is to identify and

*hxu@tsinghua.edu.cn

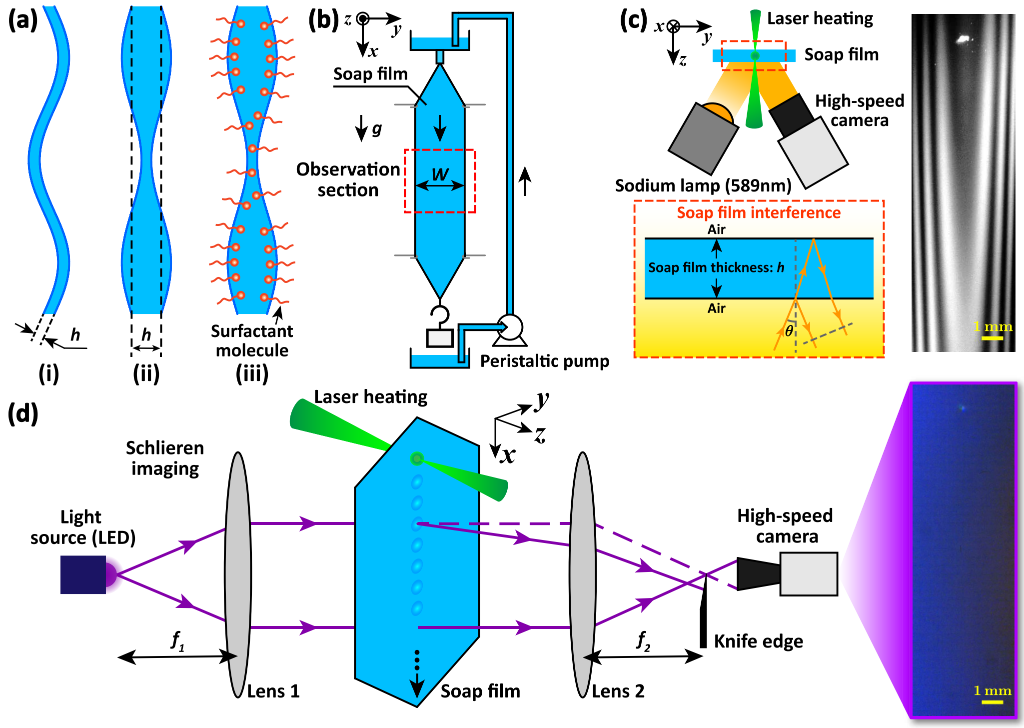

FIG. 1. (a) Schematics of waves on liquid films: (i) antisymmetric Taylor waves, (ii) symmetric Taylor waves, and (iii) symmetric elastic waves. (b) Sketch of the gravity-driven flowing soap film setup. The soap-film flow was confined by two nylon wires held by weights and four hooks. The peristaltic pump circulated the soap solution and set its volume flow rate. (c) Top view of the optical setup of the interferometry imaging (left) and an example interference image (right) of the undisturbed high-concentration ($c = 2\%$) flowing soap film. (d) Schematics of the optical setup of the Schlieren imaging and an example Schlieren image (right) taken simultaneously with the interference image shown in (c).

study the properties of the antisymmetric Taylor waves and the symmetric elastic waves in flowing soap films [23–29].

Experimentally, it has long been very difficult to isolate the antisymmetric modes from the symmetric modes, leading to long-term confusion in the understanding of these waves. For example, the view that an intrusion in a fast-flowing soap film causes symmetric elastic waves was pervasive [27,29], until it was shown in a recent study [23] that those waves actually were the antisymmetric Taylor waves. While this confusion was cleared, it motivates a renewed search for the elusive symmetric elastic waves in soap films [28], in which the main hindrance is the lack of an experimental approach to stimulate only the symmetric disturbances without triggering the antisymmetric waves.

In this letter, we propose a method of focused laser heating to introduce nonintrusive thermal stimulation [30] in the flowing film, which can produce symmetric disturbances in the film thickness without perturbing the film shape antisymmetrically. To demonstrate this idea experimentally, we constructed a flowing soap film driven by gravity and confined by two nylon wires held at a fixed separation of $W = 35$ mm in the observation section, as shown in Fig. 1(b). With a film thickness of $h \sim 10\,\mu$m, it thus formed a two-dimensional (2D) flow tunnel. The liquid used was a soap-water solution with the mass concentration $c = 2\%$ of the added DAWN detergent, which is the “standard recipe” commonly used in soap-film flow studies [7–9,19–23,27–29,31,32]. As illustrated in Figs. 1(c) and 1(d), the laser beam, with a wavelength of 532 nm and a maximum instantaneous power of $P = 6.76$ W, was focused perpendicularly on a point in the film. To increase the absorption of the visible laser by the soap film, the soap solution was mixed with 2% noncarbon black ink. The other ingredients were 2% detergent, 10% glycerol, and deionized water, all by mass. Due to the laser radiation energy absorbed by the soap film, the local temperature of the heated spot is about 10 °C higher than the surrounding film and consequently, the surface tension of the heated spot is lower. This surface tension difference drives the Marangoni flow, i.e., the soap solution at the heated spot is partially drawn into the surrounding unheated film area. Such laser-induced thermocapillary flows occur simultaneously on both surfaces of the soap film, producing symmetric patterns of reduced film thickness, as shown in the careful measurement of the film thickness change due to laser heating on a vertical standing soap film [33] (see Sec. I of the Supplemental Material [34] for detailed discussions of the film temperature rise and the thickness change caused by the laser heating).

To study the symmetric elastic wave due to the elasticity of the soap film, a closer examination of the surface tension of the film is required as the definition $E = A(d\sigma/dA)$ suggests. The surface tension of a soap film depends on the surface concentration of surfactants, which is at a balance with the bulk concentration c_1 of the surfactants in the interior of the film. When the film is stretched, the surface area increases and hence, surfactants migrate from the interior to the surface until a new balance is reached. When the bulk concentration c_1 of the surfactant is below its critical micelle concentration (CMC), i.e., in the low-concentration regime, the surface tension of the soap film decreases dramatically with the increase of the surfactant concentration. In the high-concentration regime ($c_1 >$ CMC), the surface tension is saturated to a constant [35–39]. Since the elasticity of the soap film depends on the change in surface tension as the film is stretched, the elasticity in the high-concentration regime is theoretically much lower than that in the low-concentration regime. For the effective surfactant (sodium dodecyl sulfate, SDS) in the DAWN detergent, its CMC value corresponds to $c \approx 0.5\%$ of the detergent in the soap solution [40]. Thus, at the above "standard recipe," i.e., $c = 2\%$, the surfactant is in the high-concentration regime and the propagation speed of the symmetric elastic waves will become vanishingly small, which enhances the stability of the films.

According to our analysis presented above, the spots of reduced film thickness created by the laser heating should remain on the film and simply flow with the film without propagating around. To verify this prediction, the flowing soap film was observed by interferometry and Schlieren imaging simultaneously. For interferometry, as sketched in Fig. 1(c), the soap film was illuminated by the monochromatic light (589 nm in wavelength) from a low-pressure sodium lamp. The lamp and a high-speed camera were placed on one side of the soap film and at the same angle θ with respect to the normal direction of the film. Each bright or dark fringe on the interference image, formed by interference between the reflected light from the two liquid-air interfaces of the film, corresponds to an isopach of the soap film thickness. An example interference image of the undisturbed soap film at a flow rate of $Q = 25$ ml/min and a flow speed of $u = 1.75$ m/s is shown in Fig. 1(c) next to the optical setup. The Schlieren system consisted of a white-light LED, two long-focal-length lenses, a sharp knife edge, and a high-speed camera, as sketched in Fig. 1(d). The Schlieren images reveal the deviation of the parallel light along the path [41,42], which is caused by the change of reflective index in the media or in our case, the variations in film thickness or shape. Figure 1(d) also shows an example Schlieren image of the undisturbed soap film taken simultaneously with the interference image shown in Fig. 1(c). More details of the Schlieren imaging system are described in the Supplemental Material [34].

Figure 2(a) shows the interference (left) and Schlieren (right) images when the laser was programed to output a series of pulses with a pulse frequency of $f_{\text{laser}} = 3500$ Hz, a duty cycle of 20%, and an average power of $P_{\text{ave}} = 1.35$ W. Each laser pulse induced a small pit on the soap film through the thermal-Marangoni effect. These pits, however, did not stimulate any antisymmetric wave as in the case of inserting a rod into the film at the same soap film conditions [23]. Nor were any appreciable symmetric waves, which would appear as film thickness variations, observed, except perhaps very slow growth of the size of the pits through the symmetric Taylor waves with a very small propagation speed for thin films as discussed earlier. Instead, a chain of small pits

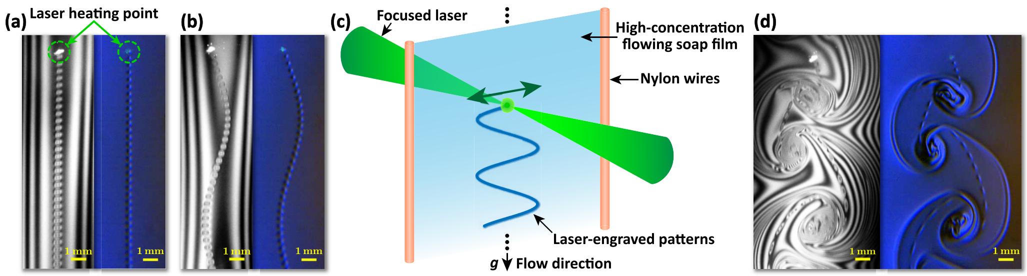

FIG. 2. (a) Interference (left) and Schlieren (right) images of the soap film shown in Fig. 1 perturbed by laser heating at a pulsing frequency of $f_{\text{laser}} = 3500\,\text{Hz}$. (b) Interference (left) and Schlieren (right) images of the same soap film when the laser beam was vibrating horizontally at 115 Hz. (c) A sketch showing how the flowing soap film records the motion of the laser focusing point. (d) Interference (left) and Schlieren (right) images of the von Kármán vortex street behind a rod inserted in the soap film, on which dots printed by a stationary pulsed laser formed a streak line in this complex 2D flow.

flowed neatly downstream with the soap film. The dynamics process when the laser pulse train was just switched on can be seen in video 1 of the Supplemental Material [34]. This interesting experimental phenomenon, which is similar to "print" or to "engrave" patterns on free liquid films by laser, provides a clear validation of the vanishingly small elasticity of the high-concentration soap films. It is worth to note that in an earlier work, Emile & Emile [33] used laser heating to trigger the Marangoni flow that resulted in local thinning in a vertical draining film with surfactant concentration "well above the critical micellar concentration." The local film thickness decreases remained on the film for considerable periods without propagating. This is consistent with our analysis above because the elasticity of the soap film with high surfactant concentration vanishes, hence thickness perturbations cannot be propagated in the form of elastic waves.

In addition, more complex patterns can also be "engraved" on the flowing soap film. Figure 2(b) (also video 2 of the Supplemental Material [34]) shows a sinusoidal curve created by letting the laser beam vibrate horizontally at 115 Hz. As sketched in Fig. 2(c), the flowing soap film acted like a "paper tape" in a seismometer, recording on the film surface the motion of the laser focusing point. Not only on flat films as shown in Figs. 2(a) and 2(b), this "laser engraving" can also be used to print patterns on a soap film with its own thickness variations. Figure 2(d) are interference and Schlieren images of the von Kármán vortex street behind a round rod inserted in the soap film, with a series of dots printed by a stationary pulsed laser (see also video 3 in the Supplemental Material [34]). Note that the instantaneous positions of these dots form a so-called streak line, which marks the fluid that passed a fixed point at earlier times and is a very common way of flow visualization. Following the trajectories of individual dots, we would also obtain the Lagrangian information of the flow, which is traditionally available only by adding tracer particles in the flow [43,44]. From this point of view, this phenomenon also offers a technique for flow visualization and Lagrangian study in complex 2D flows without tracer particles.

As we discussed earlier, for the symmetric elastic waves to appear, the soap film must possess appreciable elasticity E, which, according to $E = A(d\sigma/dA)$, means that the surfactant concentration must be below CMC so that the film surface tension is not fixed at the constant value corresponding to saturated surfactants, in opposite to the cases for "laser engraving" shown above. In the low-concentration regime, however, the surface tension of the soap film is higher. For the soap films with higher surface tension to be stable, we used a narrower tunnel with a test section width $W = 7.4\,\text{mm}$. The film thickness varied with the flow rate but was approximately $h \sim 40\,\mu\text{m}$, which made interference imaging not suitable and thus only Schlieren images were taken. Figure 3(a) and video 4 of the Supplemental Material [34] show the Schlieren images of the heating by a pulsed laser at various repetition frequencies on a soap film with a detergent mass concentration of $c = 0.057\%$,

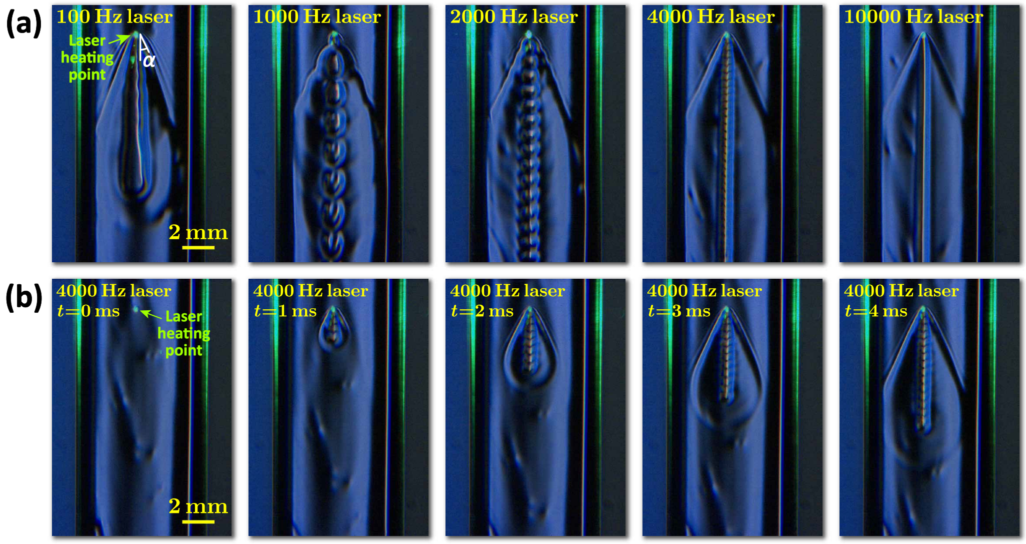

FIG. 3. Schlieren images of shock waves stimulated by pulsed laser heating with a duty cyle of 50% and an average power of $P_{\text{ave}} = 3.38$ W on a flowing soap film with a low concentration of detergent ($c = 0.057\%$). (a) For laser pulsing frequencies in the range 100 Hz $< f_{\text{laser}} <$ 10 000 Hz, shock waves formed and their Mach angles were measured to be $\alpha = 26^\circ$, independent of f_{laser}. (b) The growth process (within 4 ms) of the shock wave stimulated by the laser heating at the pulse frequency 4000 Hz.

which is well in the concentration range that the surface tension varies significantly with detergent concentration (see the data of surface tension in Fig. 4). For all laser repetition frequencies, the laser-induced disturbances in the film thickness could no longer remain unchanged with the film flow and were propagated by the symmetric elastic waves. At this film flow speed, the envelope of these wave fronts formed a shock wave starting from the laser heating point with an apparent Mach angle $\alpha = \arcsin(1/Ma) = \arcsin(v_E/u)$, i.e., the half-angle of the Mach cone, where $Ma = u/v_E$ is the Mach number. For the soap film shown in Fig. 3, the flow rate is set at $Q = 35$ ml/min, the film flowing velocity is measured at $u = 1.95$ m/s, and the film thickness is $h = Q/Wu = 40$ μm. The measured Mach angle remains the same at $\alpha = 26^\circ$, independent of the laser pulsing frequency. The propagation speed of the symmetric elastic waves is thus calculated to be $v_E = u \sin\alpha = 0.85$ m/s and the corresponding film elasticity can be calculated to be $E = \frac{1}{2}\rho h v_E^2 = 15.1$ mN/m. Furthermore, in Fig. 3(b) (see also video 5 of the Supplemental Material [34]), the growth process of the shock wave stimulated by the laser heating at the pulse frequency 4000 Hz is shown, which, despite being a 2D flow of liquid film, bears a close resemblance to the classical aerodynamic shock waves. This type of shocklike flows stimulated by laser heating on flowing soap films, which is reported for the first time, demonstrates the compressibility of soap-film flows with low surfactant concentration, in opposite to the incompressibility of soap-film flows with high surfactant concentration (see Sec. III of the Supplemental Material [34] for detailed discussions).

Further insight on the properties of the symmetric elastic waves can be gained by examining the same experiment with different detergent concentrations in the low-concentration regime (A summary of the behavior of the soap films with different detergent concentrations under different laser-heating frequencies is given in the Sec. IV of the Supplemental Material [34]). Figure 4(a) presents the Schlieren images at $c = 0.042\%$, 0.057%, and 0.078% at the same flow rate and laser pulsing frequency. Obviously, the phenomena are qualitatively the same, i.e., the formation of shock waves due to the symmetric elastic waves (see also video 6 of the Supplemental Material [34]). Quantitatively, the Mach angle α varies with the detergent concentration, with the one at $c = 0.057\%$ larger than the other two. The film elasticities calculated from the measured Mach

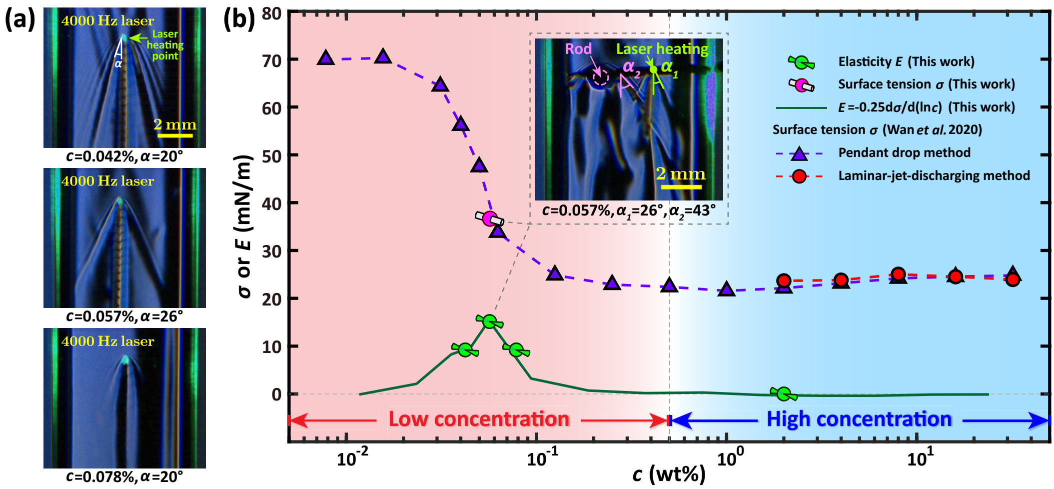

FIG. 4. Effects of detergent concentration on the behavior of flowing soap films. (a) Schlieren images of the soap films with $c = 0.042\%$, 0.057%, and 0.078%, respectively, at the same flow rate of $Q = 35\,\mathrm{ml/min}$ and the same laser pulsing frequency of $f_{\mathrm{laser}} = 4000\,\mathrm{Hz}$ with a duty cycle of 50% and an average laser power of $P_{\mathrm{ave}} = 3.38\,\mathrm{W}$. (b) Variations of the surface tension σ and film elasticity E with detergent concentrations c. The surface tension data (purple triangles and red circles) are measured by Wan *et al.* [39]. The film elasticities (green symbols) are calculated from the measured Mach angles, together with the result from the semiempirical formula $E = -0.25\mathrm{d}\sigma/\mathrm{d}(\ln c)$ (green curve). The inset shows the Schlieren image of the comparative experiment, in which a rod was inserted in the soap film with a detergent concentration $c = 0.057\%$ and at the same time a laser heating with $f_{\mathrm{laser}} = 5000\,\mathrm{Hz}$ was applied on the soap film at the same height as the rod.

angles are shown by the green data symbols in Fig. 4(b), together with the surface tension measured by Wan *et al.* [39]. A semiempirical model can be used to estimate the film elasticity from the surface tension data: $E = \frac{\mathrm{d}\sigma}{\mathrm{d}\ln A} = \frac{\mathrm{d}\ln c}{\mathrm{d}\ln A}\frac{\mathrm{d}\sigma}{\mathrm{d}\ln c} \approx B\frac{\mathrm{d}\sigma}{\mathrm{d}\ln c}$, where $B = \frac{\mathrm{d}\ln c}{\mathrm{d}\ln A}$ is approximately a constant (see Sec. V of the Supplemental Material [34]). The elasticity given by the semiempirical formula with $B = -0.25$ is shown as the green curve in Fig. 4(b), which is in good agreement with the measured elasticity. The result of this semiempirical formula suggests that the film elasticity is only appreciable for soap films with detergent concentration in the range $0.02\% \lesssim c \lesssim 0.1\%$, beyond which the film elasticity is so low that the propagation of the symmetric elastic waves cannot be clearly observed.

A unique feature of soap films with low surfactant concentration is that they allow both fast-propagating waves: the symmetric elastic waves shown above by laser heating and the antisymmetric Taylor waves that can be stimulated by intrusions [23]. The image in the middle of Fig. 4(b) shows the Schlieren imaging of the soap film with detergent concentration $c = 0.057\%$ under simultaneous perturbations of a focused laser heating and an intrusion (in this case a round rod inserted into the flowing film). Two shock waves with different Mach angles formed on the film at the same time. The Mach angle $\alpha_1 = \arcsin(v_E/u)$ of the shock corresponding to the laser heating, which is the same as shown in Fig. 4(a) when the soap film with the same detergent concentration was stimulated by laser heating alone, is smaller than the Mach angle $\alpha_2 = \arcsin(v_{AS}/u)$ corresponding to the intrusion, from which the propagation speed of the antisymmetric Taylor waves is determined to be $v_{AS} = 1.33\,\mathrm{m/s}$. The surface tension calculated from the wave speed, $\sigma = \frac{1}{2}\rho h v_{AS}^2$, is shown by the magenta symbol in Fig. 4(b), which agrees well with the surface tension data from direct measurement [39] and thus provides further evidence that the shock wave with Mach angle α_2 results from the antisymmetric Taylor waves. The coexistence of the symmetric and the antisymmetric waves clearly demonstrates the interesting properties of different waves on liquid films.

Finally, we discuss the effect of heat transfer on our analysis of wave propagation. In our analysis, we neglected the heat conduction in the soap film from the heated spot, which is justified if the timescale for heat conduction $W^2/4\beta$ is much longer than the timescale for wave propagation $W/2v_E$, i.e., when the dimensionless number $v_E W/2\beta \gg 1$, where W is the tunnel width and β is the thermal diffusivity of the liquid. For our case, a simple calculation shows that $v_E W/2\beta \approx 2\times10^4$, and thus it is allowed to neglect the heat conduction in the soap film.

In summary, we have demonstrated the laser-induced thermocapillary flows on flowing soap films with different surfactant concentrations. The key element of this laser-heating approach is to stimulate only the symmetric disturbances in the film thickness without triggering the antisymmetric waves. For the low-concentration flowing soap films, the observation of the symmetric elastic waves fills a major gap in the study of soap films, especially for the understanding of the soap film elasticity, and gives a new type of shock waves in 2D flows similar to those in aerodynamics. In the high-concentration regime, a "laser engraving" technique was proposed, which can be used to create various patterns on free liquid films without propagating and has potential applications in, e.g., performing Lagrangian studies in 2D flows without tracer particles. It is expected that the laser-heating approach will find further applications in the study of various capillary flows.

We are thankful to Dr. Zeyou Zhou for his contribution in the setup of the soap-film flow facility. This work is supported partially by the Natural Science Foundation of China (NSFC) through Grant No. 11988102 and by Tsinghua University.

[1] M. Quirk and J. Serda, *Semiconductor Manufacturing Technology* (Prentice Hall, New Jersey, 2001)

[2] A. Patsyk, U. Sivan, M. Segev, and M. A. Bandres, Observation of branched flow of light, Nature (London) **583**, 60 (2020).

[3] A. T. Oratis, J. W. M. Bush, H. A. Stone, and J. C. Bird, A new wrinkle on liquid sheets: Turning the mechanism of viscous bubble collapse upside down, Science **369**, 685 (2020).

[4] J. C. Bird, R. de Ruiter, L. Courbin, and H. A. Stone, Daughter bubble cascades produced by folding of ruptured thin films, Nature (London) **465**, 759 (2010).

[5] G. Debrégeas, P.-G. de Gennes, and F. Brochard-Wyart, The life and death of "bare" viscous bubbles, Science **279**, 1704 (1998).

[6] R. da Silveira, S. Chaïeb, and L. Mahadevan, Rippling instability of a collapsing bubble, Science **287**, 1468 (2000).

[7] J. Zhang, S. Childress, A. Libchaber, and M. Shelley, Flexible filaments in a flowing soap film as a model for one-dimensional flags in a two-dimensional wind, Nature (London) **408**, 835 (2000).

[8] S. Alben, M. Shelley, and J. Zhang, Drag reduction through self-similar bending of a flexible body, Nature (London) **420**, 479 (2002).

[9] T. Tran, P. Chakraborty, N. Guttenberg, A. Prescott, H. Kellay, W. Goldburg, N. Goldenfeld, and G. Gioia, Macroscopic effects of the spectral structure in turbulent flows, Nat. Phys. **6**, 438 (2010).

[10] A. Vilquin, J. Jagielka, S. Djambov, H. Herouard, P. Fischer, C.-H. Bruneau, P. Chakraborty, G. Gioia, and H. Kellay, Asymptotic turbulent friction in 2D rough-walled flows, Sci. Adv. **7**, eabc6234 (2021).

[11] L. Shen, F. Denner, N. Morgan, B. van Wachem, and D. Dini, Transient structures in rupturing thin films: Marangoni-induced symmetry-breaking pattern formation in viscous fluids, Sci. Adv. **6**, eabb0597 (2020).

[12] A. Oron, S. H. Davis, and S. G. Bankoff, Long-scale evolution of thin liquid films, Rev. Mod. Phys. **69**, 931 (1997).

[13] G. I. Taylor, The dynamics of thin sheets of fluid II. Waves on fluid sheets, Proc. R. Soc. London, Ser. A **253**, 296 (1959).

[14] J. Lucassen, M. Van den Tempel, A. Vrij, and F. Hesselink, Waves in thin liquid films I. The different modes of vibrations, Proc. K. Ned. Akad. Wet. B **73**, 109 (1970).

[15] A. Vrij, F. Hesselink, J. Lucassen, and M. Van den Tempel, Waves in thin liquid films II. Symmetrical modes in very thin films and film ruptures, Proc. K. Ned. Akad. Wet. B **73**, 124 (1970).

[16] Y. Couder, J. M. Chomaz, and M. Rabaud, On the hydrodynamics of soap films, Physica D **37**, 384 (1989).

[17] N. Bremond and E. Villermaux, Atomization by jet impact, J. Fluid Mech. **549**, 273 (2006).
[18] B. Néel and E. Villermaux, The spontaneous puncture of thick liquid films, J. Fluid Mech. **838**, 192 (2018).
[19] M. A. Rutgers, X. L. Wu, and W. B. Daniel, Conducting fluid dynamics experiments with vertically falling soap films, Rev. Sci. Instrum. **72**, 3025 (2001).
[20] H. Kellay and W. I. Goldburg, Two-dimensional turbulence: A review of some recent experiments, Rep. Prog. Phys. **65**, 845 (2002).
[21] G. Boffetta and R. E. Ecke, Two-dimensional turbulence, Annu. Rev. Fluid Mech. **44**, 427 (2012).
[22] Z. Y. Zhou, L. Fang, N. T. Ouellette, and H. T. Xu, Vorticity gradient stretching in the direct enstrophy transfer process of two-dimensional turbulence, Phys. Rev. Fluids **5**, 054602 (2020).
[23] Y. Zhao and H. T. Xu, Observation of antisymmetric shock waves in soap-film flows, Phys. Rev. Fluids **7**, L082001 (2022).
[24] C. Y. Wen, Y. M. Chen, and S. K. Chang-Jian, A soap film shock tube to study two-dimensional compressible flows, Exp. Fluids **31**, 19 (2001).
[25] C. Y. Wen and J. Y. Lai, Analogy between soap film and gas dynamics. I. Equations and shock jump conditions, Exp. Fluids **34**, 107 (2003).
[26] C. Y. Wen, S. K. Chang-Jian, and M. C. Chuang, Analogy between soap film and gas dynamics. II. Experiments on one-dimensional motion of shock waves in soap films, Exp. Fluids **34**, 173 (2003).
[27] T. Tran, P. Chakraborty, G. Gioia, S. Steers, and W. I. Goldburg, Marangoni shocks in unobstructed soap-film flows, Phys. Rev. Lett. **103**, 104501 (2009).
[28] I. Kim and X. L. Wu, Tunneling of micron-sized droplets through soap films, Phys. Rev. E **82**, 026313 (2010).
[29] I. Kim and S. Mandre, Marangoni elasticity of flowing soap films, Phys. Rev. Fluids **2**, 082001(R) (2017).
[30] Y. Zhao, D. M. Wan, X. L. Chen, X. Chao, and H. T. Xu, Uniform breaking of liquid-jets by modulated laser heating, Phys. Fluids **33**, 044115 (2021).
[31] M. Rivera, P. Vorobieff, and R. E. Ecke, Turbulence in flowing soap films: Velocity, vorticity, and thickness fields, Phys. Rev. Lett. **81**, 1417 (1998).
[32] T. Schnipper, A. Andersen, and T. Bohr, Vortex wakes of a flapping foil, J. Fluid Mech. **633**, 411 (2009).
[33] J. Emile and O. Emile, Mapping of the Marangoni effect in soap films using Young's double-slit experiment, Europhys. Lett. **104**, 14001 (2013).
[34] See Supplemental Material http://link.aps.org/supplemental/10.1103/PhysRevFluids.9.L022001 for the analysis of the temperature increase and film thickness reduction at the laser-heated spot, the details of the Schlieren imaging system, the incompressibility of soap-film flows with high detergent concentrations, the responses of soap films to laser-heating, the elasticity of soap films, and Supplemental Videos 1–6.
[35] H. Bianco and A. Marmur, Gibbs elasticity of a soap bubble, J. Colloid Interface Sci. **158**, 295 (1993).
[36] F. Evans and W. Wennerström, *The Colloidal Domain* (Wiley, New York, 1999).
[37] D. Langevin and F. Monroy, Marangoni stresses and surface compression rheology of surfactant solutions. achievements and problems, Adv. Colloid Interface Sci. **206**, 141 (2014).
[38] D. Langevin, Rheology of adsorbed surfactant monolayers at fluid surfaces, Annu. Rev. Fluid Mech. **46**, 47 (2014).
[39] D. M. Wan, H. S. Xiang, and H. T. Xu, A laminar-jet-discharging method for measuring the interfacial tension of deformable surfaces, Meas. Sci. Technol. **31**, 035302 (2020).
[40] A. Sane, S. Mandre, and I. Kim, Surface tension of flowing soap films, J. Fluid Mech. **841**, R2 (2018).
[41] G. S. Settles, *Schlieren and Shadowgraph Techniques* (Springer, Berlin, 2001).
[42] C. Tropea, A. L. Yarin, and J. Foss, *Springer Handbook of Experimental Fluid Mechanics* (Springer, Berlin, 2007).
[43] M. Bourgoin, N. T. Ouellette, H. Xu, J. Berg, and E. Bodenschatz, The role of pair dispersion in turbulent flow, Science **311**, 835 (2006).
[44] F. Toschi and E. Bodenschatz, Lagrangian properties of particles in turbulence, Annu. Rev. Fluid Mech. **41**, 375 (2009).